PCCP

Exceptional H2 Sorption Characteristics in a Mg2+-Based Metal–Organic Framework with Small Pores: Insights From Experimental and Theoretical Studies

Journal:	*Physical Chemistry Chemical Physics*
Manuscript ID	CP-ART-10-2015-005906.R1
Article Type:	Paper
Date Submitted by the Author:	04-Dec-2015
Complete List of Authors:	Eckert, Juergen; University of South Florida, Department of Chemistry Space, Brian; University of South Florida, Chemistry Forrest, Katherine; University of South Florida, Chemistry Pham, Tony; University of South Florida, Chemistry Falcao, Eduardo; Universidade Federal de Pernambuco, Departamento de Quimica Fundamental

Exceptional H_2 Sorption Characteristics in a Mg^{2+}-Based Metal–Organic Framework with Small Pores: Insights From Experimental and Theoretical Studies

Tony Pham,[†] Katherine A. Forrest,[†] Eduardo H. L. Falcão,[‡] Juergen Eckert,[*,†] and Brian Space[*,†]

[†]*Department of Chemistry, University of South Florida, 4202 East Fowler Avenue, CHE205, Tampa, FL 33620-5250, United States*

[‡]*Departamento de Química Fundamental, Universidade Federal de Pernambuco, Av. Jorn. Anibal Fernandes, s/n, Cidade Universitária, Recife, PE, 50740-560, Brazil*

ABSTRACT: Experimental sorption measurements, inelastic neutron scattering (INS), and theoretical studies of H_2 sorption were performed in α–$[Mg_3(O_2CH)_6]$, a metal–organic framework (MOF) that consists of a network of Mg^{2+} ions coordinated to formate ligands. The experimental H_2 uptake at 77 K and 1.0 atm was observed to be 0.96 wt %, which is quite impressive for a Mg^{2+}-based MOF that has a BET surface area of only 150 m^2 g^{-1}. Due to the presence of small pore sizes in the MOF, the isosteric heat of adsorption (Q_{st}) value was observed to be reasonably high for a material with no open-metal sites (*ca.* 7.0 kJ mol^{-1}). The INS spectra for H_2 in α–$[Mg_3(O_2CH)_6]$ is very unusual for a porous material, as there exist several different peaks that occur below 10 meV. Simulations of H_2 sorption in α–$[Mg_3(O_2CH)_6]$ revealed that the H_2 molecules sorbed at three principal locations within the small pores of the framework. It was discovered through the simulations and two-dimensional quantum rotation calculations that different groups of peaks correspond to particular sorption sites in the material. However, for H_2 sorbed at a specific site, it was observed that differences in the positions and angular orientations led to distinctions in the rotational tunnelling transitions; this led to a total of eight identified sites. An extremely high rotational barrier was calculated for H_2 sorbed at the most favorable site in α–$[Mg_3(O_2CH)_6]$ (81.59 meV); this value is in close agreement to that determined using an empirical phenomenological model (75.71 meV). This rotational barrier for H_2 exceeds those for various MOFs that contain open-metal sites and is currently the highest yet for a neutral MOF. This study highlights the synergy between experiment and theory to extract useful and important atomic level details on the remarkable sorption mechanism for H_2 in a MOF with small pore sizes.

I. INTRODUCTION

Metal–organic frameworks (MOFs) represent a class of porous materials that are synthesized by combining metal ions with organic ligands in a symmetric, periodic fashion.[1,2] These materials have been considered to be promising for applications in H_2 storage.[3–5] Their porous nature allows for the possibility to store a sizeable amount of H_2 molecules within the pores. In addition, because H_2 sorption in MOFs is based on physisorption, these materials have the ability to release the H_2 molecules easily through changes in thermodynamic conditions. Since 2003,[6] a number of different MOFs have been investigated for their H_2 uptake capacity.[5] Benchmark studies of H_2 sorption on MOFs are usually performed at 77 K and low pressures (e.g., up to 1.0 atm). Although MOFs can sorb a significant quantity of H_2 at 77 K, the H_2 uptake in these materials are very low at room temperature and high pressure.[4] Continuous research is being done to find ways to increase the H_2 uptake capacity and associated adsorption enthalpy in MOFs, since one of the major goals in this energy economy is to synthesize a suitable material that is appropriate for on-board H_2 storage at near-ambient temperatures. Numerous earlier experimental studies have shown that MOFs that contain open-metal sites,[7–9] narrow pore sizes,[10–12] nitrogen-rich centers,[13–15] and/or counterions[16,17] usually display greater affinity for H_2.

MOFs are highly tunable as myriad different structures can be synthesized or predicted by changing the metal ion and/or ligand.[18,19] In 2006, a Mg^{2+}-based MOF was synthesized by combining $Mg(NO_3)_2$ with formic acid in dimethylformamide (DMF) at elevated temperatures.[20] Removal of the guest DMF molecules upon activation yielded a stable, solvent-free material known as α–$[Mg_3(O_2CH)_6]$ (Figure 1). The resulting structure consists of an extended network in which each Mg^{2+} ion is bonded to the surrounding oxygen atoms of the formate ligands in an octahedral fashion (i.e., MgO_6). Note, MOFs based on Mg^{2+} appear to be very attractive for the purposes of H_2 storage because of their low densities in cases where the organic linker is coordinated directly to the metal as observed in α–$[Mg_3(O_2CH)_6]$. However, efforts to synthesize additional Mg^{2+}-based MOFs with larger pores (excluding Mg-MOF-74)[9] were unsuccessful because the framework would collapse upon solvent evacuation, since the Mg^{2+} ions (unlike transition metal cations) have flexible coordination geometries.[21,22]

As shown in Figure 1, the crystal structure of α–$[Mg_3(O_2CH)_6]$ contains four Mg^{2+} ions that are in chemically distinguishable environments; they are denoted Mg1, Mg2, Mg3, and Mg4 in this manuscript. The Mg1 and Mg4 ions are both connected to four μ_1–O and two μ_2–O atoms, whereas the Mg2 ion is connected to six μ_1–O atoms and the Mg3 ion is connected to two μ_1–O and four μ_2–O atoms. Further, the Mg2 and Mg3 ions represent edge-shared octahedra that are linked together by vertex-shared octahedra (the Mg1 and Mg4 ions). In addition, there are six chemically distinct formate linkers in the crystal structure of α–$[Mg_3(O_2CH)_6]$ (see Supporting Information, Figure S2).

α–$[Mg_3(O_2CH)_6]$ consists of very small accessible pores that can be viewed along the *b*-axis of the crystal structure (Figure 1(b)). The windows of the channels are approximately 4.5 Å × 5.5 Å wide based on the van der Waals radii of the atoms. Experimental studies have shown that these pores can be used to sorb a variety of small guest molecules. In order to elucidate the effect of the small pores in α–$[Mg_3(O_2CH)_6]$ on the affinity of the MOF to H_2 molecules, we carried out a joint experimental and theoretical study of the H_2 sorption mechanism in α–$[Mg_3(O_2CH)_6]$.

H_2 gas sorption measurements were conducted on α–

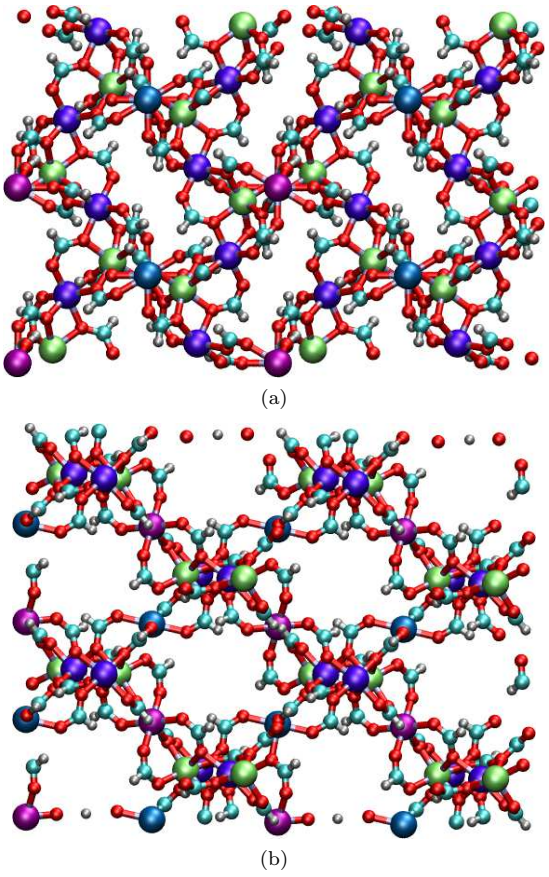

Figure 1. (a) The orthographic *a*-axis and **(b)** *b*-axis views of the 2 × 2 × 2 system cell of α–$[Mg_3(O_2CH)_6]$. The Mg^{2+} ions are color-coded to highlight the four chemically distinct Mg^{2+} ions. Atoms colors: C = cyan, H = white, O = red, Mg1 = magenta, Mg2 = lime green, Mg3 = violet, Mg4 = blue.

$[Mg_3(O_2CH)_6]$ at low temperatures and pressures and the resultant experimental H_2 sorption isotherms and isosteric heat of adsorption (Q_{st}) are presented in this work. We also performed inelastic neutron scattering (INS) studies for H_2 sorbed in this MOF to obtain molecular level information on the binding sites in the framework. INS is a useful spectroscopic technique that is used to gain insights into the energetics and rotational barriers for H_2 sorbed in MOFs and other porous materials.[23] The resulting INS spectra contain a relatively large number of distinct peaks from transitions of the hindered H_2 rotor, where typically each rotational tunnelling transition corresponds to a certain H_2 sorption site in the material. Peaks that occur at lower energies correspond to a higher barrier to rotation, and therefore, a stronger interaction with the host, whereas the opposite is true for peaks occurring at higher energies.

Molecular simulations of H_2 sorption in α–$[Mg_3(O_2CH)_6]$ were also performed in this work to obtain atomistically detailed insights into the H_2 sorption mechanism and to identify the favorable sorbate binding sites in the MOF. In addition, two-dimensional quantum rotation calculations were executed for the discovered H_2 sorption sites in α–$[Mg_3(O_2CH)_6]$. These calculations were carried out in an attempt to make assignments of the various peaks that are present in the INS spectra. Indeed, these quantum dynamics calculations can provide a nice complement to the INS experiments.[12,24] Insights into the rotational barrier for H_2 sorbed at the most favorable site in α–$[Mg_3(O_2CH)_6]$ was also obtained in this work. We note that while experimental H_2 sorption measurements in α–$[Mg_3(O_2CH)_6]$ were carried out more recently by a different group,[25] this manuscript reports the first INS and computational study of H_2 sorption in this MOF.

II. METHODS

A. Experimental Section

α–$[Mg_3(O_2CH)_6]$ was synthesized and activated according to the procedure reported in reference 20. The experimental H_2 sorption isotherms for α–$[Mg_3(O_2CH)_6]$ at 77 and 87 K and pressures up to 1.0 atm were acquired using a Micromeritics ASAP 2010 surface area and porosity analyzer. The H_2 Q_{st} values were obtained by applying the Clausius–Clapeyron equation[26] to the experimental isotherms at both temperatures.

The INS spectra for α–$[Mg_3(O_2CH)_6]$ were collected at a temperature of 10 K on the QENS spectrometer at the Intense Pulsed Neutron Source (IPNS) of Argonne National Laboratory. Successful loading of the material with amounts of H_2 related to the number of formula units in the sample was carried out *in situ* at 77 K after first obtaining a spectrum of the "blank" sample. The sample was equilibrated after loading before cooling to the data collection temperature of 10 K. The spectra shown for α–$[Mg_3(O_2CH)_6]$ in this work were obtained by subtracting the "blank" spectrum.

B. Computational Section

H_2 sorption simulations in α–$[Mg_3(O_2CH)_6]$ were executed using grand canonical Monte Carlo (GCMC)[27] on the 2 × 2 × 2 system cell of the MOF as shown in Figure 1. Here, the sorbate molecules were randomly inserted, deleted, or moved (translated or rotated) in a simulation box containing the MOF–H_2 system. This process continued for a number of Monte Carlo steps until equilibrium was reached for desired state points. The chemical potential, volume, and temperature of the system were kept constant for simulations at various pressure reservoirs. Periodic boundary conditions were applied to model an infinite crystalline environment for the α–$[Mg_3(O_2CH)_6]$ structure. A spherical cutoff corresponding to half the shortest system cell dimension length was used for the simulations. In addition, all MOF atoms were held rigid throughout the simulations.

The chemical potentials for H_2 at the temperatures and pressures considered in this work were calculated using the BACK equation of state.[28] The total potential energy for the MOF–H_2 system was calculated by summing the repulsion/dispersion and electrostatic energies. These energetic terms were calculated through the Lennard-Jones 12–6 potential and Ewald summation[29] of the partial charges, respectively. Note, our group frequently includes the explicit polarization term to the potential energy function for classical simulations of gas sorption in MOFs.[30–37] However, α–$[Mg_3(O_2CH)_6]$ is a MOF containing very narrow pore sizes, which allows for van der Waals interactions to dominate. Smaller pores in MOFs would allow for multiple atoms of the framework to interact with the sorbate molecules simultaneously, thus producing an attractive van der Waals well.

As a result, explicit induction interactions were negligible for H_2 sorption in α–$[Mg_3(O_2CH)_6]$. Indeed, control simulations in α–$[Mg_3(O_2CH)_6]$ including polarization interactions revealed that this energetic term contributed to roughly 2% of the total energy for all state points considered and does not significantly alter the simulated H_2 sorption isotherms and Q_{st} values. Similar findings were also observed for simulations of H_2 sorption in other MOFs with small pore sizes.[38–40]

To treat quantum effects for H_2 at the temperatures considered herein, Feynman-Hibbs corrections to the fourth order were applied to the potential energy.[41] The average particle number for each state point considered was calculated numerically using a statistical mechanical expression that is based on the grand canonical ensemble.[42] This value was then converted to a quantity that represents the H_2 uptake in the experimental sorption isotherm. In GCMC, the Q_{st} values were calculated using an expression based on the fluctuations of the particle number and total potential energy.[43] For all state points considered, the simulations initially consisted of 2.5×10^6 Monte Carlo steps to reach equilibrium. Afterward, the simulations continued for an additional 2.5×10^6 Monte Carlo steps to sample the desired thermodynamic properties.

Simulated annealing calculations[44] within the canonical ensemble (NVT) were also performed on the MOF–H_2 system to identify all of the H_2 sorption sites in the MOF. The simulations were performed in the $2 \times 2 \times 2$ system cell of α–$[Mg_3(O_2CH)_6]$ at H_2 saturation. An initial temperature of 1,000 K was selected for the simulated annealing calculations, and this temperature was scaled by a factor of 0.99999 after every 1,000 Monte Carlo steps. The simulation continued until the temperature dropped below 5.0 K. Afterward, the H_2 molecules located at the global minimum as well as various local minima were identified in α–$[Mg_3(O_2CH)_6]$.

Two-dimensional quantum rotation calculations were executed for H_2 molecules sorbed at certain sites in α–$[Mg_3(O_2CH)_6]$ that were determined from the simulated annealing calculations. As with the aforementioned simulations, the quantum rotation calculations were carried out using the $2 \times 2 \times 2$ system cell of the MOF. The quantum rotation calculations involve solving the rigid rotor Hamiltonian for the MOF–H_2 system for each sorption site of interest as described and implemented previously by our group (see Supporting Information).[12,24,32–37] Further, the rotational potential energy surface for H_2 sorbed at the most favorable site in α–$[Mg_3(O_2CH)_6]$ was calculated in this work and details for computing this are provided in the Supporting Information. All simulations and quantum rotation calculations in α–$[Mg_3(O_2CH)_6]$ were performed using the Massively Parallel Monte Carlo (MPMC) code, an open-source code that is available for download on GitHub.[45]

All MOF atoms were treated with Lennard-Jones parameters (ϵ and σ) and point partial charges. The ϵ and σ values for the Mg and O atoms were taken from the Universal Force Field (UFF),[46] while those for C and H were taken from the Optimized Potentials For Liquid Simulations – All Atom (OPLS-AA) force field.[47] The partial charges for the chemically distinct atoms in α–$[Mg_3(O_2CH)_6]$ were determined through periodic fitting of the entire crystal structure using the Vienna *ab initio* Simulation Package (VASP)[48–51] with the projector augmented wave (PAW) method[52] and Ceperley–Alder (CA) functional.[53] A restraining potential was implemented to treat the presence of buried atoms in the structure. The calculations were performed using a charge fitting code that was developed previously.[54,55] The resulting calculated partial charges are provided in the Supporting Information (Table S1). For the sorbate model, the five–site electrostatic (nonpolarizable) potential that was developed previously by Belof *et al.*[56] was used for the H_2 sorption simulations.

III. RESULTS AND DISCUSSION

A. Isotherms and Isosteric Heats of Adsorption

The experimental H_2 sorption isotherms in α–$[Mg_3(O_2CH)_6]$ at 77 and 87 K and pressures up to 900 torr are shown in Figure 2(a). Due to the small surface area and pore size of α–$[Mg_3(O_2CH)_6]$, the H_2 uptake in this MOF is quite limited, with a value of 0.96 wt % of H_2 at 77 K and 1.0 atm. Note, wt % is defined as: [(Mass of H_2)/(Mass of MOF + Mass of H_2)] × 100%. However, this value for the H_2 uptake in α–$[Mg_3(O_2CH)_6]$ at 77 K and 1.0 atm is still remarkable for a MOF that has a BET surface area of only 150 m^2 g^{-1}.[20]. As a comparison, the H_2 uptake value in Mg-MOF-74 reaches about 2.5 wt% at the same state point with nearly 12 times the BET surface area.[9] In addition, the aforementioned H_2 uptake value for α–$[Mg_3(O_2CH)_6]$ is higher than that for Mg-MOF-1, another Mg^{2+}-based MOF containing open-metal sites, under the same conditions (0.70 wt %).[57] The isotherms at both temperatures display a noticeable rise in the H_2 uptakes at pressures below 100 torr, which could indicate a reasonably high H_2 Q_{st} value for this MOF containing no open-metal sites or other charged/polar moieties.

Figure 2(b) shows the H_2 Q_{st} values as a function of H_2 uptake for α–$[Mg_3(O_2CH)_6]$. These Q_{st} values were derived by applying the Clausius–Clapeyron equation[26] to the experimental H_2 sorption isotherms at 77 and 87 K. The H_2 Q_{st} values are nearly constant at *ca.* 7.0 kJ mol^{-1} for all loadings considered. These Q_{st} values are similar to those reported for this MOF in previous work, with the same general shape across the loading range.[25] The shape of the Q_{st} plot suggests homogeneity in the H_2 binding sites or a number of different sites having similar adsorption enthalpies. In addition, this Q_{st} value for α–$[Mg_3(O_2CH)_6]$ is greater than or comparable to some MOFs that possess open-metal sites.[8,58] While the Q_{st} plot for α–$[Mg_3(O_2CH)_6]$ is mostly flat, the plots for a number of MOFs containing open-metal sites (e.g., HKUST-1, PCN-61) exhibit a monotonically decreasing behavior as a function of loading.

The simulated H_2 sorption isotherms at 77 and 87 K for α–$[Mg_3(O_2CH)_6]$ as compared to the corresponding experimental data are provided in the Supporting Information (Figure S4(a)). The simulated sorption isotherms are in good agreement with experiment to within joint uncertainties for the considered pressure range (0–1 atm) at both temperatures. The slight oversorption compared to experiment for nearly all pressures considered at both temperatures could be due to the fact that the simulations utilize a perfect crystal of the MOF, whereas slight impurities may be present in the actual synthesized crystals.

GCMC simulations predict H_2 Q_{st} values in α–$[Mg_3(O_2CH)_6]$ that are slightly higher than experiment (*ca.* 7.5 kJ mol^{-1}) (see Supporting Information, Figure S4(b)). The simulations also captured the same general shape for the Q_{st} plot as experiment, where the Q_{st} values are virtually

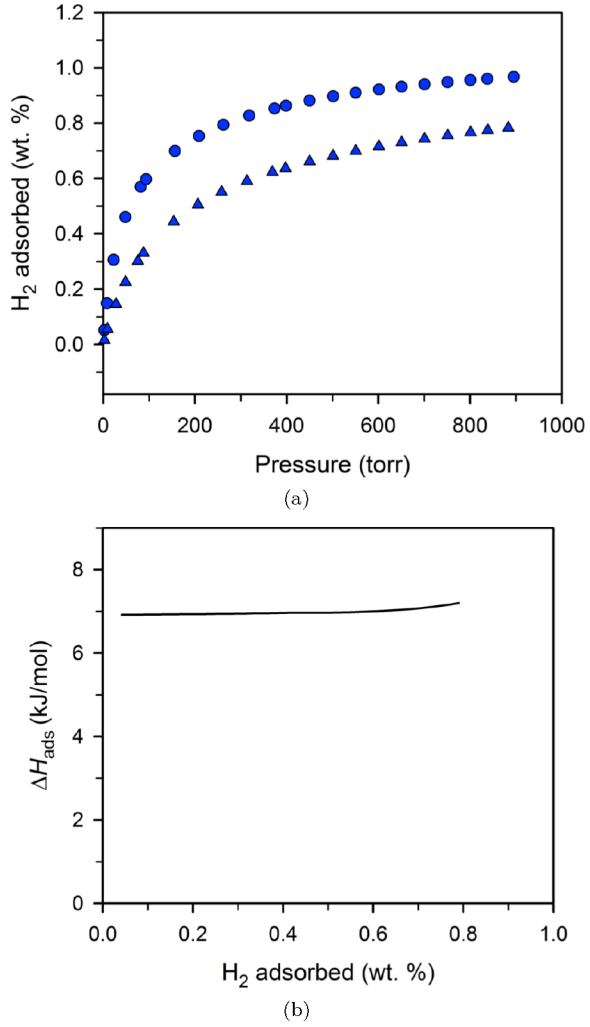

Figure 2. **(a)** Experimental H_2 sorption isotherms for α–$[Mg_3(O_2CH)_6]$ at 77 K (circles) and 87 K (triangles). **(b)** Isosteric heat of adsorption (Q_{st}) for H_2 plotted against H_2 uptakes for α–$[Mg_3(O_2CH)_6]$.

constant for all H_2 uptakes considered. Further, the modeling studies predict that H_2 saturation is reached in the MOF at about 1.15 wt %, which is in agreement to what was observed in previous experimental measurements.[25] Outstanding agreement with experimental measurements for the sorption observables allows for confidence in molecular level predictions of the sorption sites in the MOF. Note, it can be observed from the experimental and simulated Q_{st} plots that the Q_{st} increases slightly as the H_2 uptake approaches saturation in the MOF. This increase in the Q_{st} could be due to H_2–H_2 interactions as the pores are getting filled up in the material.

B. Inelastic Neutron Scattering Spectra

The INS spectra for H_2 sorbed in α–$[Mg_3(O_2CH)_6]$ is shown in Figure 3 at different loadings (0.12, 0.25, and 0.40 H_2 molecules per formula unit). The spectra were collected on the QENS spectrometer at the neutron source IPNS of Argonne National Laboratory. Interestingly, the INS spectra for the MOF reveals eight peaks occurring at approximately

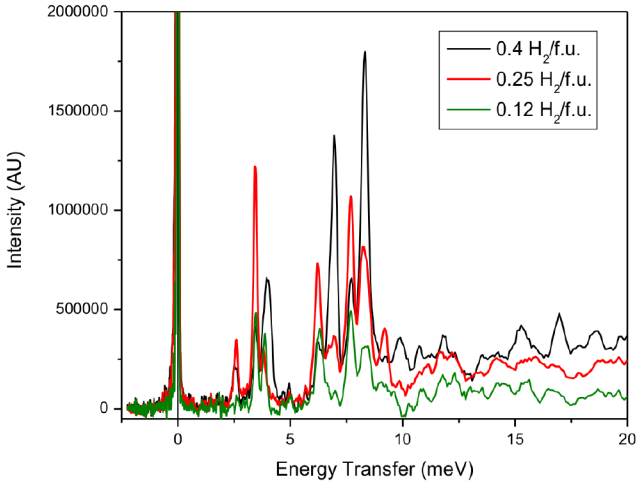

Figure 3. Inelastic neutron scattering (INS) spectra for H_2 in α–$[Mg_3(O_2CH)_6]$ at different loadings: 0.12 H_2/formula unit (green), 0.25 H_2/formula unit (red), and 0.40 H_2/formula unit (black). The spectra were collected on the QENS spectrometer at the neutron source IPNS of Argonne National Laboratory.

2.5, 3.4, 3.9, 6.2, 6.9, 7.7, 8.3, and 9.2 meV. Notable differences in the intensities of these peaks can be observed at the various loadings. To the best of our knowledge, these spectra for H_2 sorbed in α–$[Mg_3(O_2CH)_6]$ exhibit the largest number of clearly defined rotational tunnelling transitions and energies well below the rigid rotor limit (14.7 meV) out of any MOFs based on previous INS studies. Further, all of the transitions occur below 10 meV, with three of them appearing below 5 meV. This indicates that nearly all H_2 molecules that are sorbed in α–$[Mg_3(O_2CH)_6]$ are highly rotationally hindered. The existence of eight peaks in the INS spectra for α–$[Mg_3(O_2CH)_6]$ suggests that there are eight unique H_2 sorption sites in the MOF. It will be shown later that certain groups of peaks in the spectra correspond to particular locations in the MOF, but with slightly different positions and angular orientations for the sorbate molecules.

The peak at 2.5 meV in the INS spectra for α–$[Mg_3(O_2CH)_6]$, which is observed at 0.25 and 0.40 H_2 molecules per formula unit, is much lower than the lowest energy peaks that appear in the INS spectra for a number of MOFs, especially those that contain open-metal sites or extra-framework counterions. Indeed, the value of this rotational transition is lower than those observed for MOFs that contain $[Cu_2(CO_2R)_4]$ units,[33,59–62] members of the M-MOF-74 series,[9,63,64] and certain MOFs that contain counterions.[16,17,32] This peak at 2.5 meV corresponds to a rotational barrier of 75.71 meV according to an empirical phenomenological model based on a simple double-minimum potential.[65] This value for the rotational barrier is one of the highest that exists in the literature for H_2 sorbed in a porous material and it is currently the highest for a neutral MOF. In addition, the rotational barrier for H_2 in α–$[Mg_3(O_2CH)_6]$ is only marginally lower than that observed for the most favorable H_2 sorption site in the anionic rare-earth **fcu**-MOF Y-FTZB.[35] It will be shown below that the H_2 sorption site that gives rise to the 2.5 meV peak in α–$[Mg_3(O_2CH)_6]$ produces a calculated rotational barrier that is comparable to the aforementioned empirical value.

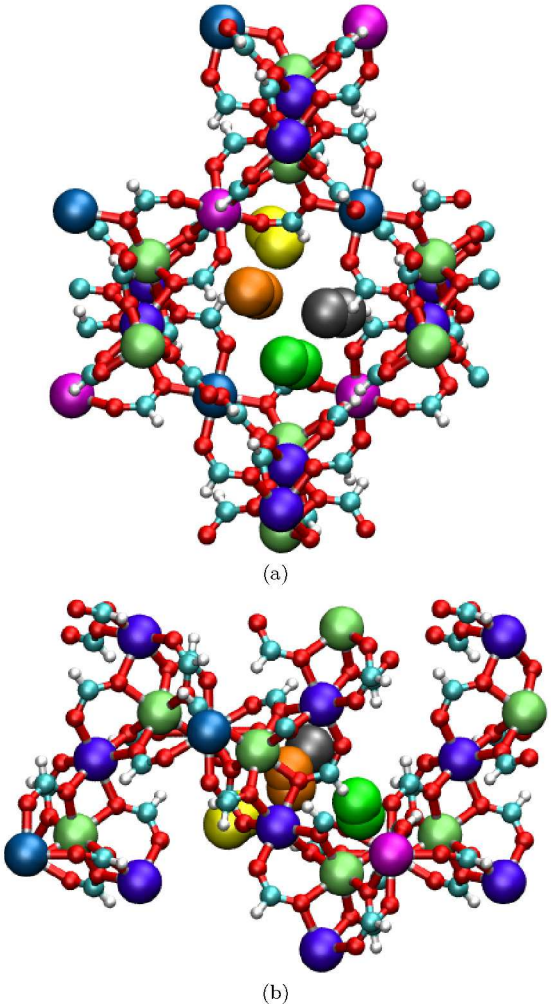

Figure 4. Molecular illustration of the sorbed H_2 molecules within the pores of α–$[Mg_3(O_2CH)_6]$ as determined from simulation: **(a)** *b*-axis view and **(b)** *a*-axis view. The H_2 molecules and Mg^{2+} ions are color-coded to highlight the different H_2 sorption sites and chemically distinct Mg^{2+} ions, respectively. H_2 molecule colors: site 1A = green, site 1B = yellow, site 2A = orange, site 2B = gray. Atoms colors: C = cyan, H = white, O = red, Mg1 = magenta, Mg2 = lime green, Mg3 = violet, Mg4 = blue. Note, sites 1B and 2B are reflected on the opposite side of the pore from sites 1A and 2A, respectively, for illustrative purposes.

C. Identification of H_2 Sorption Sites

1. Site 1

Simulated annealing calculations for H_2 sorbed in α–$[Mg_3(O_2CH)_6]$ revealed that the most favorable sorption site in the MOF (i.e., the global minimum) corresponds to a confined region at one side of the pore (enclosed by the Mg1, Mg2, and Mg4 ions) where the positively charged H atoms of the H_2 molecule can interact with the nearby negatively charged O atoms of the formate linkers (Figure 4). Indeed, in this region, the H_2 molecule can interact with at least eight different O atoms from the surrounding formate linkers. The closest distance between a H atom of the H_2 molecule and one of the O atoms of the framework was measured to be 2.34 Å (Figure S8(a)). Two-dimensional quantum rotation calculations for a H_2 molecule sorbed about this site, denoted site 1A in this work, produced a 0 to 1 transition of 2.57 meV. This calculated rotational level is extremely close to the transition energy of the lowest energy peak in the INS spectra for the MOF (2.5 meV). Note, all calculated rotational levels for the considered H_2 sorption sites in α–$[Mg_3(O_2CH)_6]$ in this work are provided in the Supporting Information (Table S3). In addition, a comparison of the experimental rotational tunnelling transitions (as observed in the INS spectra) to the calculated 0 to 1 transitions for the different H_2 sorption sites considered in α–$[Mg_3(O_2CH)_6]$ are summarized in Table 1.

Table 1. The rotational tunnelling transitions (in meV) observed in the inelastic neutron scattering (INS) spectra (Figure 3) compared the calculated 0 to 1 transitions through two-dimensional quantum rotation calculations for the different H_2 sorption sites in α–$[Mg_3(O_2CH)_6]$. Sites 1A, 1B, 2A, and 2B are depicted in Figure 4, while site 1C is depicted in Figure 6, and sites 3A, 3B, and 3C are depicted in Figure 7.

Site	Experiment (meV)	Calculated (meV)
1A	2.5	2.57
1B	3.4	4.19
1C	3.9	4.54
2A	6.2	6.48
2B	6.9	7.07
3A	7.7	8.08
3B	8.3	8.80
3C	9.2	9.18

Next, the rotational potential energy surface for a H_2 molecule sorbed at site 1A was calculated and the plot is shown in Figure 5. According to Figure 5, the rotational barrer was estimated to be 81.59 meV, which is in good agreement with the previously mentioned value that was determined using a phenomenological model (75.71 meV). This confirms that the rotational barrier for H_2 sorbed at site 1A is tremendously high, as it is, to the best of our knowledge, the highest within any neutral MOF based on a literature survey of INS studies on MOFs.[35] Apparently, the interactions from several different oxygen atoms within a constricted region cause this H_2 molecule to exhibit an extremely high rotational barrier. Currently, the only MOF that displays a higher rotational barrier for H_2 than that for the most favorable sorption site in α–$[Mg_3(O_2CH)_6]$ is Y-FTZB.[35] It was shown in previous theoretical studies on Y-FTZB that a H_2 molecule sorbed onto an accessible Y^{3+} ion, nitrogen atoms of tetrazolate groups, and a $(CH_3)_2NH_2^+$ counterion simultaneously in the MOF corresponded to a rotational barrier of 85.77 meV; this value is slightly higher than that for a H_2 molecule sorbed at site 1A in α–$[Mg_3(O_2CH)_6]$ in this work.

The 2.5 meV peak is absent in the INS spectra at the lowest loading measured (0.12 H_2/formula unit), but it is present in the spectra with fairly low intensity at 0.25 H_2/formula unit and 0.4 H_2/formula unit. The low intensity of the 2.5 meV peak signifies that only a small number of H_2 molecules are sorbed at this site for the loadings considered. This suggests that site 1A is difficult to access even though it is the most favorable site in the structure. The transition occurring at about 3.4 meV in the INS spectra for α–$[Mg_3(O_2CH)_6]$ represents the highest intensity peak at a loading of 0.25 H_2/formula unit. The peak at approximately 3.9 meV is noticeable at 0.12 H_2/formula unit and the intensity of this peak is increased by roughly a factor of two

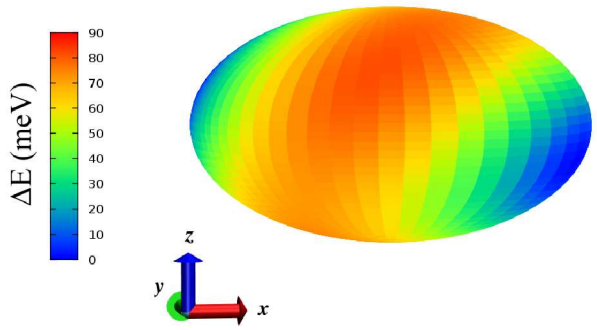

Figure 5. Two-dimensional rotational potential energy surface projected onto a sphere for a H_2 molecule sorbed about the most favorable site in α–$[Mg_3(O_2CH)_6]$ (site 1A) as shown in Figure 4. Relative energies are given in meV. The rotational barrier was calculated to be 81.59 meV.

by 0.40 H_2/formula unit.

The simulations in this work revealed H_2 sorption sites that are very similar to that for site 1A and, although slightly less energetically favorable than site 1A, are quite populated in the MOF throughout all loadings. This is consistent with observations for the 3.4 and 3.9 meV peaks in the INS spectra (i.e., very strong binding sites that are comparable to site 1A in energetics and are prevalent at all loadings). For one of the sites, denoted site 1B herein, the H_2 molecule is positioned slightly farther away from the O atoms of the formate linkers and is oriented differently (Figure 4). The shortest distance measured between a H atom of the H_2 molecule and one of the framework O atoms was 2.53 Å (Figure S8(b)). Because the H_2 molecule is mildly farther away from the negatively charged O atoms of the linkers, the transition energy for the sorbate molecule is increased marginally (i.e., the rotational barrier decreases). As for the other site, denoted site 1C herein, this H_2 molecule has nearly the same orientation about the designated side of the pore as site 1A, but it is positioned reasonably farther away from the O atoms of the formate linkers (Figure 6). The H_2 molecule sorbed at site 1C is also mildly farther away from of the O atoms of the linkers than that at site 1B, thus indicating a minimally higher rotational transition energy and slightly less interactions. The closest H(H_2)–O(MOF) distance for this site was observed to be 2.59 Å (Figure S8(c)).

For H_2 molecules sorbed at sites 1B and 1C, 0 to 1 transitions of 4.19 and 4.54 meV were calculated for the individual sites, which are reasonably near 3.4 and 3.9 meV, respectively (see Table 1). In essence, sites 1A, 1B, and 1C correspond to one principal location in the MOF (site 1), where the H_2 molecule is sorbed in the compact area between the formate linkers at the side of the pore enclosed by the Mg1, Mg2, and Mg4 ions in the MOF. The only differences between these three sites are minor changes in the position and orientation. It is expected that the presence of other H_2 molecules in the pore would allow those molecules sorbed at sites 1B and 1C to move closer to a more energetically favorable position between the formate linkers, thus allowing site 1A to exist. This could explain why the 2.5 meV peak exists at the two highest loadings measured, but not at 0.12 H_2/formula unit. Further, it can be observed that the intensity of the 3.4 meV peak decreases dramatically from 0.25 H_2/formula unit to 4.0 H_2/formula unit, whereas the opposite is observed for the 3.9 meV peak at the same loadings. This could indicate that, at loadings beyond 0.25 H_2/formula unit, the H_2 molecules that are sorbed at site 1B are dynamically transitioning to site 1C as more H_2 molecules enter the MOF.

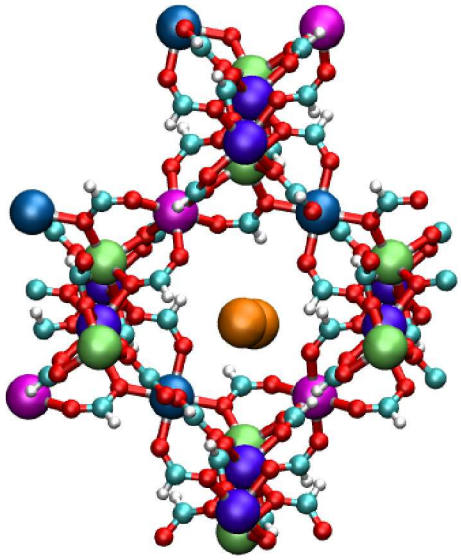

Figure 6. Molecular illustration of the sorbed H_2 molecule within the pore of α–$[Mg_3(O_2CH)_6]$ as determined from simulation. The H_2 molecule (orange) shown is sorbed at site 1C. The Mg^{2+} ions are color-coded to highlight the four chemically distinct Mg^{2+} ions. Atoms colors: C = cyan, H = white, O = red, Mg1 = magenta, Mg2 = lime green, Mg3 = violet, Mg4 = blue.

2. *Site 2*

The simulations revealed that the H_2 molecules can also sorb at the side of the pore that is enclosed by the Mg2 and Mg3 ions in α–$[Mg_3(O_2CH)_6]$; it is denoted site 2 in this work (Figure 4). This region is adjacent to the side of the pore that accommodates site 1. The H_2 molecules that are sorbed at site 2 are located farther along the *b*-axis compared to those H_2 molecules that are sorbed at site 1 (Figure 4(b)). Within the region for site 2, the H_2 molecules can interact with at least four different O atoms from the surrounding formate linkers. Two different subsites were observed for site 2 in which the H_2 molecule positions and orientations are slightly different; they are denoted sites 2A and 2B, respectively (Figure 4).

The H_2 molecule that is sorbed at site 2A is positioned closer to more of the O atoms of the formate linkers and therefore, it is slightly more favorable. Two-dimensional quantum rotation calculations produced a rotational level of 6.48 meV for the 0 to 1 transition for this site. This value for the calculated rotational transition is in close agreement with the transition energy for the peak occurring at about 6.2 meV in the INS spectra for the MOF. This 6.2 meV peak has a fairly high intensity in the spectra at 0.25 H_2/formula unit and it represents the fourth strongest H_2 sorption site in the material overall.

For the H_2 molecule that is sorbed at site 2B, which is located somewhat farther away from a lot of the O atoms of the formate linkers and has a slightly different orientation compared to that at site 2A, a 0 to 1 transition of 7.07 meV was calculated for this site. This value is very close to the peak appearing at about 6.9 meV in the INS spec-

tra for α–$[Mg_3(O_2CH)_6]$. Although the 6.9 meV peak is almost nonexistent at 0.12 H_2/formula unit and has a small intensity at 0.25 H_2/formula unit, the magnitude of this peak is very large at 0.40 H_2/formula unit. In addition, it can be observed that the 6.2 meV peak exhibits higher intensity than the 6.9 meV peak at the two lowest loadings measured, but at 0.40 H_2/formula unit, the intensity of the 6.9 meV peak becomes very large, while the intensity of 6.2 meV peak decreases notably from 0.25 H_2/formula unit to 0.40 H_2/formula unit. This indicates that sorption at site 2A is more prevalent than at site 2B at low loadings, but as the loading increases, site 2B becomes the dominant sorption site among the two subsites for site 2. Further, it is speculated that the H_2 molecules that are sorbed at site 2A are dynamically transitioning to site 2B at higher loadings when more H_2 molecules are introduced into the MOF; this could explain why the population of H_2 molecules sorbed at site 2A is reduced from 0.25 H_2/formula unit to 0.40 H_2/formula unit and why site 2B is highly populated at the the highest loading measured. Note, although the H atoms of the H_2 molecule is very close to one of the O atoms of the framework for site 2B, these H atoms are noticeably farther away from the other surrounding O atoms (Figure S9(b)).

The quantum rotation calculations performed herein have confirmed that sorption at site 2A is more energetically favorable than sorption at site 2B since a lower transition energy was calculated for the former. Because the H_2 molecules at site 2 can only interact closely with four oxygen atoms from the neighboring formate linkers compared to eight oxygen atoms in the case of site 1, the rotational transition is increased to higher energies as observed in the INS spectra and quantum rotation calculations. Due to the transition energies of the two peaks occurring at nearly 6.2 and 6.9 meV and the fact that the calculated rotational levels for H_2 molecules sorbed at site 2 (i.e., sorption into the region located at the side of the pore in which the Mg2 and Mg3 ions line the pore walls) are close to the aforementioned transitions, we have assigned the peaks at 6.2 and 6.9 meV to be associated with sorption at sites 2A and 2B, respectively.

3. Site 3

Apart from the sides of the pores in α–$[Mg_3(O_2CH)_6]$, the H_2 molecules were also found to localize toward the center of the pores of the MOF according to the simulations (Figure 7). The region near the center of the pore, denoted site 3 in this work, represents a weaker binding site in the MOF than the sides of the pores since the H_2 molecules are typically farther away from the oxygen atoms on the ligands. Three different subsites were observed for site 3 in α–$[Mg_3(O_2CH)_6]$. The majority of measured distances between the H atoms of the H_2 molecule and the nearby O atoms of the framework for these sites are greater than 3.0 Å (Figure S10). The most favorable H_2 molecule position for site 3 is actually located in the area between the two adjacent sides of the pores that accommodate sites 1 and 2, respectively (Figure 7(a)). A H_2 molecule that is positioned at this site, denoted site 3A herein, is somewhat close to the nearby oxygen atoms of the formate ligands. However, because this H_2 molecule is farther away from the linkers compared to those H_2 molecules that are sorbed at sites 1 and 2, the rotational frequency for this molecule increases (meaning weaker interactions). Indeed, a rotational level of 8.08 meV was calculated for this site for the lowest transition from the quantum rotation calculations. This value is in good agreement with the peak occurring at approximately 7.7 meV in the INS spectra for α–$[Mg_3(O_2CH)_6]$, which is the next highest energy peak after the 6.9 meV peak. The high relative intensity of the 7.7 meV peak at 0.12 H_2/formula unit and 0.25 H_2/formula unit signifies a large occupancy of H_2 molecules sorbing at site 3A in this MOF for the low loadings considered.

The H_2 molecules sorbed at the other two subsites for site 3 in α–$[Mg_3(O_2CH)_6]$ are positioned much closer to the center of the pore than a H_2 molecule sorbed at site 3A. For site 3B, the H_2 molecule is sorbed very close to center of the pore, but is oriented perpendicular to the *b*-axis (Figure 7(b)). On the other hand, the H_2 molecule sorbed at site 3C is located at the same place as site 3B, but the sorbate molecule is oriented parallel with respect to the *b*-axis (Figure 7(c)). Because of the orientation of the H_2 molecule sorbed at site 3B, the sorbate molecule can interact slightly with the oxygen atoms of the formate ligands across the pore, thus providing for mildly greater interactions with the MOF than the H_2 molecule sorbed at site 3C. The H_2 molecule cannot interact significantly with the framework when it is sorbed at site 3C.

The notion that site 3B is more favorable than site 3C was verified through quantum rotation calculations, as a H_2 molecule sorbed at site 3B displayed a lower rotational energy for the 0 to 1 transition than that sorbed at site 3C (8.80 vs. 9.18 meV). These calculated values are actually in close agreement with the transition energies for the peaks appearing at about 8.3 and 9.2 meV, respectively, in the INS spectra for α–$[Mg_3(O_2CH)_6]$. It can be observed that the 8.3 meV peak exhibits the highest intensity throughout the entire INS spectra for the MOF at 4.0 H_2/formula unit, thus implying that the majority of H_2 molecules are sorbed at site 3B at this loading. This is consistent with what was observed from the simulations at high loadings. Note, a pattern similar to that observed between the 6.2 and 6.9 meV peaks can be seen when comparing the 7.7 and 8.3 meV peaks for the different loadings. Further, site 3C is not as favorable for the sorbed H_2 molecules as compared to the other sorption sites in α–$[Mg_3(O_2CH)_6]$. This could explain why the intensity of the 9.2 meV peak is very low across all loadings considered.

Due to the positions of the peaks at 7.7, 8.3, and 9.2 meV, the relative energetics of the H_2 molecules sorbed at site 3, and the close agreement between the experimental and calculated transitions, we have assigned the peaks occurring at 7.7, 8.3, and 9.2 meV to be associated with H_2 molecules sorbing at sites 3A, 3B, and 3C, respectively. Note, despite higher transition energies for H_2 molecules sorbed at site 3 relative to sites 1 and 2, these rotational transitions are still similar to those observed for sorption onto the $[Cu_2(O_2CR)_4]$ clusters in MOFs that contain such units (e.g., HKUST-1, PCN-12, *rht*-MOF-4a).[59,61,62] This indicates that even the weakest H_2 sorption sites in α–$[Mg_3(O_2CH)_6]$ are comparably rotationally hindered to H_2 molecules sorbed onto an open-metal Cu^{2+} ion of a copper paddlewheel.

IV. CONCLUSION

A combined experimental and theoretical study of H_2 sorption was performed in α–$[Mg_3(O_2CH)_6]$, a Mg^{2+}-based MOF containing very small pore sizes. Although the H_2 uptake in the MOF was found to be quite low at 77 K and 1.0 atm (0.96 wt %), especially compared to other MOFs that

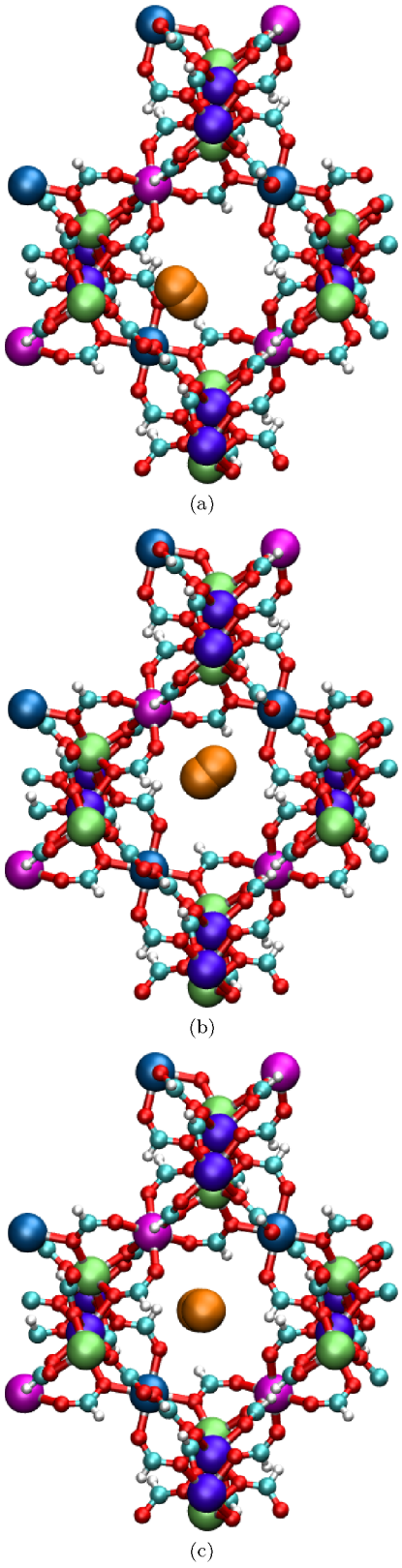

Figure 7. Molecular illustration of the sorbed H_2 molecules within the pore of α–$[Mg_3(O_2CH)_6]$ as determined from simulation. The H_2 molecules (orange) shown are sorbed at site 3.**(a)** site 3A, **(b)** site 3B, and **(c)** site 3C. The Mg^{2+} ions are color-coded to highlight the four chemically distinct Mg^{2+} ions. Atoms colors: C = cyan, H = white, O = red, Mg1 = magenta, Mg2 = lime green, Mg3 = violet, Mg4 = blue.

exhibit much higher H_2 uptake capacities at the same state point,[5] this value is still remarkable for a material that has a BET surface area of only 150 m^2 g^{-1}.[20] The derived Q_{st} value (*ca.* 7.0 kJ mol^{-1}) is comparable to those for some MOFs that contain open-metal sites,[8,58] thus demonstrating the effect of small pore sizes on the H_2 sorption energetics in MOFs. The constant H_2 Q_{st} values observed for all loadings considered for α–$[Mg_3(O_2CH)_6]$ suggests homogeneity in the binding sites. However, the INS spectra for H_2 at different loadings in the MOF revealed at least eight different peaks from transitions of the hindered H_2 rotor. All of these peaks occur below 10 meV, with three of them appearing below 5 meV, and this represents an unusual finding in the case of H_2 sorbed in porous materials. The simulations executed herein assisted in the identification of the H_2 sorption sites in α–$[Mg_3(O_2CH)_6]$. The simulations revealed that the H_2 molecules are sorbed at three main locations in the MOF: (1) the side of the pore that encloses the Mg1, Mg2, and Mg4 ions, (2) the side of the pore that encloses the Mg2 and Mg3 ions, and (3) towards the center of the pore. However, differences in the positions and angular orientations cause the rotational tunnelling transitions of the H_2 molecules at these sites to alter. As a result, a total of eight different sites were observed in this work for α–$[Mg_3(O_2CH)_6]$.

The two-dimensional quantum rotation calculations performed herein on the considered H_2 sorption sites in α–$[Mg_3(O_2CH)_6]$ revealed rotational tunnelling transitions that were in good agreement with those that were observed in the INS spectra of the MOF. Indeed, these calculations on the various H_2 sorption sites assisted in the predictive interpretation of a very complex INS spectra. Based on the relative energetics for the discovered H_2 sorption sites from the simulations, the locations of the peaks in the spectra, and the agreement between the experimental and calculated rotational transitions for different sites, a thorough interpretation of the INS spectra for α–$[Mg_3(O_2CH)_6]$ on the basis of modeling was provided in this work. Overall, this study highlighted the power of using computational modeling to explain certain features that result from the spectroscopic measurements.

The rotational barrier for H_2 sorbed at the most favorable site in α–$[Mg_3(O_2CH)_6]$ was discovered to be very high through the experimental and theoretical studies. The preferential H_2 sorption site in the MOF is responsible for the very low energy peak occurring at approximately 2.5 meV in the INS spectra; this peak corresponds to a rotational barrier of 75.71 meV according to an empirical phenomenological model.[65] The conclusion that this H_2 molecule exhibits a high rotational barrier was supported by the theoretical studies executed herein, as calculation of the rotational potential energy surface for a H_2 molecule sorbed at this site revealed a rotational barrier of 81.59 meV. The observed rotational barrier for a H_2 molecule sorbed at the global minimum in α–$[Mg_3(O_2CH)_6]$ in this work is currently the highest of any known neutral MOF based on a literature survey of past INS studies in MOFs.[35] This value for the rotational barrier far exceeds those for MOFs that contain open-metal sites according to past INS and theoretical studies.[35,59,66] This study shows that reducing the pore sizes in MOFs is a promising route to increase the rotational barriers and sorption energetics for H_2 in porous materials. It is expected that introducing open-metal sites and/or counterions into this α–$[Mg_3(O_2CH)_6]$ system in some fashion will result in a further increase in the rotational barrier.

Our discoveries from the joint experimental and theoretical study of H_2 sorption in α–$[Mg_3(O_2CH)_6]$ demonstrate that small pore sizes are highly effective for increasing the H_2 sorpton energetics in MOFs, which in turn implies that the sorbed H_2 molecules are subject to unusually high barriers to rotation. Moreover, the nearly flat loading dependence of the H_2 Q_{st} observed for α–$[Mg_3(O_2CH)_6]$ is a critical ingredient for a potential H_2 storage system. However, the value for the H_2 adsorption enthalpy in α–$[Mg_3(O_2CH)_6]$ is too low for a practical sorption-based system operating at room temperature, for which a value of 15–30 kJ mol^{-1} is required.[67,68] We speculate that a variant of α–$[Mg_3(O_2CH)_6]$ with additional functionalities, such as open-metal sites and/or counterions, could exhibit appreciably higher H_2 Q_{st} values that could fall within the required range for a room temperature sorption-based H_2 storage system.

ASSOCIATED CONTENT

Supporting Information. Pictures of the MOF and components, tables of properties, additional H_2 sorption results, and details of quantum rotation calculations. This material is available free of charge *via* the Internet at http://pubs.acs.org.

AUTHOR INFORMATION

Corresponding Author
*E-mail: juergen@usf.edu (J.E.)
*E-mail: brian.b.space@gmail.com (B.S.)

Notes
The authors declare no competing financial interest.

ACKNOWLEDGMENTS

We would like to thank A. K. Cheetham and Z. Hulvey for helpful discussions, and R. Ziegler and N. de Souza for help with the experiment at IPNS. This work was funded in part by the Office of Energy Efficiency and Renewable Energy, U.S. Department of Energy (DE-FC36-50GO15004). B.S. acknowledges the National Science Foundation (Award No. CHE-1152362), the computational resources that were made available by a XSEDE Grant (No. TG-DMR090028), and the use of the services provided by Research Computing at the University of South Florida. This publication is also based on work supported by Award No. FIC/2010/06, made by King Abdullah University of Science and Technology (KAUST).

[1] S. L. James, *Chem. Soc. Rev.*, 2003, **32**, 276–288.
[2] H. Furukawa, K. E. Cordova, M. OKeeffe and O. M. Yaghi, *Science*, 2013, **341**, 1230444.
[3] D. Zhao, D. Yuan and H.-C. Zhou, *Energy Environ. Sci.*, 2008, **1**, 222–235.
[4] D. J. Collins, S. Ma and H.-C. Zhou, in *Metal-Organic Frameworks: Design and Application*, John Wiley & Sons, Inc., Hoboken, NJ, 2010, pp. 249–266.
[5] M. P. Suh, H. J. Park, T. K. Prasad and D.-W. Lim, *Chem. Rev.*, 2012, **112**, 782–835.
[6] N. L. Rosi, J. Eckert, M. Eddaoudi, D. T. Vodak, J. Kim, M. O'Keeffe and O. M. Yaghi, *Science*, 2003, **300**, 1127–1129.
[7] B. Chen, N. W. Ockwig, A. R. Millward, D. S. Contreras and O. M. Yaghi, *Angew. Chem. Int. Ed.*, 2005, **117**, 4823–4827.
[8] J. L. C. Rowsell and O. M. Yaghi, *J. Am. Chem. Soc.*, 2006, **128**, 1304–1315.
[9] P. D. C. Dietzel, P. A. Georgiev, J. Eckert, R. Blom, T. Strassle and T. Unruh, *Chem. Commun.*, 2010, **46**, 4962–4964.
[10] B. Kesanli, Y. Cui, M. R. Smith, E. W. Bittner, B. C. Bockrath and W. Lin, *Angew. Chem. Int. Ed.*, 2005, **44**, 72–75.
[11] S. Ma, D. Sun, M. Ambrogio, J. A. Fillinger, S. Parkin and H.-C. Zhou, *J. Am. Chem. Soc.*, 2007, **129**, 1858–1859.
[12] P. Nugent, T. Pham, K. McLaughlin, P. A. Georgiev, W. Lohstroh, J. P. Embs, M. J. Zaworotko, B. Space and J. Eckert, *J. Mater. Chem. A*, 2014, **2**, 13884–13891.
[13] B. Li, Z. Zhang, Y. Li, K. Yao, Y. Zhu, Z. Deng, F. Yang, X. Zhou, G. Li, H. Wu, N. Nijem, Y. J. Chabal, Z. Lai, Y. Han, Z. Shi, S. Feng and J. Li, *Angew. Chem. Int. Ed.*, 2012, **51**, 1412–1415.
[14] X.-J. Wang, P.-Z. Li, Y. Chen, Q. Zhang, H. Zhang, X. X. Chan, R. Ganguly, Y. Li, J. Jiang and Y. Zhao, *Sci. Rep.*, 2013, **3**, year.
[15] R. Luebke, L. J. Weselinski, Y. Belmabkhout, Z. Chen, L. Wojtas and M. Eddaoudi, *Cryst. Growth Des.*, 2014, **14**, 414–418.
[16] Y. Liu, J. F. Eubank, A. J. Cairns, J. Eckert, V. C. Kravtsov, R. Luebke and M. Eddaoudi, *Angew. Chem. Int. Ed.*, 2007, **46**, 3278–3283.
[17] F. Nouar, J. Eckert, J. F. Eubank, P. Forster and M. Eddaoudi, *J. Am. Chem. Soc.*, 2009, **131**, 2864–2870.
[18] M. Eddaoudi, D. B. Moler, H. Li, B. Chen, T. M. Reineke, M. O'Keeffe and O. M. Yaghi, *Acc. Chem. Res.*, 2001, **34**, 319–330.
[19] M. Eddaoudi and J. F. Eubank, in *Metal–Organic Frameworks: Design and Application*, John Wiley & Sons, Inc., Hoboken, NJ, 2010, pp. 37–89.
[20] J. A. Rood, B. C. Noll and K. W. Henderson, *Inorg. Chem.*, 2006, **45**, 5521–5528.
[21] K. C. Kam, K. L. M. Young and A. K. Cheetham, *Cryst. Growth Des.*, 2007, **7**, 1522–1532.
[22] Z. Hulvey and A. K. Cheetham, *Solid State Sci.*, 2007, **9**, 137–143.
[23] J. Eckert and W. Lohstroh, in *Neutron Applications in Materials for Energy*, ed. G. J. Kearley and V. K. Peterson, Springer International Publishing, 2015, pp. 205–239.
[24] I. Matanović, J. L. Belof, B. Space, K. Sillar, J. Sauer, J. Eckert and Z. Bačić, *J. Chem. Phys.*, 2012, **137**, 014701.
[25] B. Schmitz, I. Krkljus, E. Leung, H. Höffken, U. Müller and M. Hirscher, *ChemSusChem*, 2010, **3**, 758–761.
[26] H. Pan, J. A. Ritter and P. B. Balbuena, *Langmuir*, 1998, **14**, 6323–6327.
[27] N. Metropolis, A. W. Rosenbluth, M. N. Rosenbluth, A. H. Teller and E. Teller, *J. Chem. Phys.*, 1953, **21**, 1087–1092.
[28] T. Boublík, *Fluid Phase Equilibr.*, 2005, **240**, 96–100.
[29] P. P. Ewald, *Ann. Phys.*, 1921, **369**, 253–287.
[30] K. A. Forrest, T. Pham, K. McLaughlin, J. L. Belof, A. C. Stern, M. J. Zaworotko and B. Space, *J. Phys. Chem. C*, 2012, **116**, 15538–15549.
[31] T. Pham, K. A. Forrest, P. Nugent, Y. Belmabkhout, R. Luebke, M. Eddaoudi, M. J. Zaworotko and B. Space, *J. Phys. Chem. C*, 2013, **117**, 9340–9354.
[32] T. Pham, K. A. Forrest, A. Hogan, K. McLaughlin, J. L. Belof, J. Eckert and B. Space, *J. Mater. Chem. A*, 2014, **2**, 2088–2100.
[33] T. Pham, K. A. Forrest, J. Eckert, P. A. Georgiev, A. Mullen, R. Luebke, A. J. Cairns, Y. Belmabkhout, J. F. Eubank, K. McLaughlin, W. Lohstroh, M. Eddaoudi and B. Space, *J. Phys. Chem. C*, 2014, **118**, 439–456.
[34] T. Pham, K. A. Forrest, K. McLaughlin, J. Eckert and B. Space, *J. Phys. Chem. C*, 2014, **118**, 22683–22690.
[35] T. Pham, K. A. Forrest, P. A. Georgiev, W. Lohstroh, D.-X. Xue, A. Hogan, M. Eddaoudi, B. Space and J. Eckert, *Chem. Commun.*, 2014, **50**, 14109–14112.
[36] T. Pham, K. A. Forrest, R. Banerjee, G. Orcajo, J. Eckert and B. Space, *J. Phys. Chem. C*, 2015, **119**, 1078–1090.
[37] T. Pham, K. A. Forrest, A. Hogan, B. Tudor, K. McLaughlin, J. L. Belof, J. Eckert and B. Space, *Cryst. Growth Des.*, 2015, **15**, 1460–1471.
[38] A. C. Stern, J. L. Belof, M. Eddaoudi and B. Space, *J. Chem. Phys.*, 2012, **136**, 034705.
[39] T. Pham, K. A. Forrest, K. McLaughlin, B. Tudor, P. Nugent, A. Hogan, A. Mullen, C. R. Cioce, M. J. Zaworotko and B. Space, *J. Phys. Chem. C*, 2013, **117**, 9970–9982.
[40] K. A. Forrest, T. Pham, P. A. Georgiev, F. Pinzan, C. R. Cioce, T. Unruh, J. Eckert and B. Space, *Langmuir*, 2015, **31**, 7328–7336.
[41] R. P. Feynman and A. R. Hibbs, *Quantum Mechanics and Path Integrals*, McGraw-Hill, New York, 1965.
[42] D. Frenkel and B. Smit, *Understanding Molecular Simulation: From Algorithms to Applications*, Academic Press, New York, 2002.
[43] D. Nicholson and N. G. Parsonage, *Computer Simulation and the Statistical Mechanics of Adsorption*, Academic Press, London, 1982.
[44] S. Kirkpatrick, C. D. Gelatt and M. P. Vecchi, *Science*, 1983, **220**, 671–680.
[45] J. L. Belof and B. Space, *Massively Parallel Monte Carlo (MPMC)*, Available on GitHub, 2012, `https://github.com/mpmccode/mpmc`.
[46] A. K. Rappé, C. J. Casewit, K. S. Colwell, W. A. Goddard and W. M. Skiff, *J. Am. Chem. Soc.*, 1992, **114**, 10024–10035.
[47] W. L. Jorgensen, D. S. Maxwell and J. Tirado-Rives, *J. Am. Chem. Soc.*, 1996, **118**, 11225–11236.
[48] G. Kresse and J. Hafner, *Phys. Rev. B*, 1993, **47**, 558–561.
[49] G. Kresse and J. Hafner, *Phys. Rev. B*, 1994, **49**, 14251–14269.
[50] G. Kresse and J. Furthmuller, *Comput. Mater. Sci.*, 1996, **6**, 15–50.
[51] G. Kresse and J. Fürthmuller, *Phys. Rev. B*, 1996, **54**, 11169–11186.
[52] P. E. Blöchl, *Phys. Rev. B*, 1994, **50**, 17953.
[53] D. M. Ceperley and B. J. Alder, *Phys. Rev. Lett.*, 1980, **45**, 566–569.
[54] A. C. Stern, *Ph.D. thesis*, University of South Florida, 2010.
[55] D.-L. Chen, A. C. Stern, B. Space and J. K. Johnson, *J. Phys. Chem. A*, 2010, **114**, 10225–10233.
[56] J. L. Belof, A. C. Stern and B. Space, *J. Chem. Theory Comput.*, 2008, **4**, 1332–1337.
[57] A. Mallick, S. Saha, P. Pachfule, S. Roy and R. Banerjee, *J. Mater. Chem.*, 2010, **20**, 9073–9080.
[58] D. Yuan, D. Zhao, D. Sun and H.-C. Zhou, *Angew. Chem. Int. Ed.*, 2010, **122**, 5485–5489.
[59] C. M. Brown, Y. Liu, T. Yildirim, V. K. Peterson and C. J. Kepert, *Nanotechnology*, 2009, **20**, 204025.
[60] S. Ma, J. Eckert, P. M. Forster, J. W. Yoon, Y. K. Hwang, J.-S. Chang, C. D. Collier, J. B. Parise and H.-C. Zhou, *J. Am. Chem. Soc.*, 2008, **130**, 15896–15902.
[61] X.-S. Wang, S. Ma, P. Forster, D. Yuan, J. Eckert, J. López,

B. Murphy, J. Parise and H.-C. Zhou, *Angew. Chem. Int. Ed.*, 2008, **47**, 7263–7266.

[62] J. F. Eubank, F. Nouar, R. Luebke, A. J. Cairns, L. Wojtas, M. Alkordi, T. Bousquet, M. R. Hight, J. Eckert, J. P. Embs, P. A. Georgiev and M. Eddaoudi, *Angew. Chem. Int. Ed.*, 2012, **51**, 10099–10103.

[63] Y. Liu, H. Kabbour, C. M. Brown, D. A. Neumann and C. C. Ahn, *Langmuir*, 2008, **24**, 4772–4777.

[64] M. H. Rosnes, M. Opitz, M. Frontzek, W. Lohstroh, J. P. Embs, P. A. Georgiev and P. D. C. Dietzel, *J. Mater. Chem. A*, 2015, **3**, 4827–4839.

[65] J. M. Nicol, J. Eckert and J. Howard, *J. Phys. Chem.*, 1988, **92**, 7117–7121.

[66] L. Kong, G. Román-Pérez, J. M. Soler and D. C. Langreth, *Phys. Rev. Lett.*, 2009, **103**, 096103.

[67] S. K. Bhatia and A. L. Myers, *Langmuir*, 2006, **22**, 1688–1700.

[68] S. Ma, *Pure Appl. Chem.*, 2009, **81**, 2235–2251.

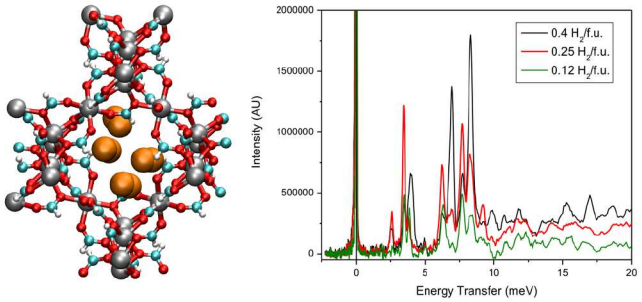

Table of Contents (TOC) Graphic: A combined experimental and theoretical study of H_2 sorption in α–$[Mg_3(O_2CH)_6]$ revealed a number of different sorption sites with distinct rotational tunnelling transitions.